Stem Cell Reports, Volume *8*

Supplemental Information

Distinct Roles for Matrix Metalloproteinases 2 and 9 in Embryonic Hematopoietic Stem Cell Emergence, Migration, and Niche Colonization

Lindsay N. Theodore, Elliott J. Hagedorn, Mauricio Cortes, Kelsey Natsuhara, Sarah Y. Liu, Julie R. Perlin, Song Yang, Madeleine L. Daily, Leonard I. Zon, and Trista E. North

SUPPLEMENTAL FIGURE LEGENDS

Figure S1. Mmp2 and Mmp9 are expressed in discrete populations within hemogenic regions.

Related to Figure 1.

A) Exposure to dimethyl-Prostaglandin-E2 (PGE2) (10μM) and CAY10397 (CAY) (10μM), a small molecule that stabilizes endogenous PGE2, increased *runx1* and *cmyb* expression in the ventral dorsal aorta (VDA) by WISH, while the cyclooxygenase antagonist Indomethacin (Indo, 10μM) decreased expression of HSPC markers at 36 hours post fertilization (hpf).

B) Qualitative phenotypic distribution of embryos from S1A scored with high/medium/low *runx1/cmyb* expression in the AGM (n≥20 embryos/condition).

C) qPCR analysis using FACS-sorted cell populations from *Tg(kdrl:dsred;cmyb:gfp)* embryos at 36 hpf showed enrichment of *mmp2* in the $Flk1^{+}cMyb^{-}$ vasculature, while *mmp9* expression was present in all populations examined (1000 embryos x 2 replicate sorts). Error bars: mean ± SD.

D) RNA-seq analysis (~1000 pooled *Tg(mpeg1:mcherry;mpx:egfp)* embryos, >50,000 cells/fraction) indicated that *mmp9* expression is concentrated in FACS-sorted Mpx^{+} neutrophils at 72 hpf.

E) Metronidozole (Mtz)-mediated (24-48 hpf) targeted ablation of primitive myeloid cell types in *Tg(mpeg1:gal4;uas:nfsb-mcherry)* (macrophage) or *Tg(mpx:gal4;uas:nfsb-mcherry)* (neutrophil) embryos confirmed that neutrophil loss strongly diminished *mmp9* expression in the trunk and tail, while macrophage loss had minimal impact.

F) Qualitative phenotypic distribution of embryos from S1E scored with high/medium/low *mmp9* expression in the trunk and tail region (n≥25 embryos/condition).

Scale bars: 100μm.

Figure S2. The pan-gelatinase inhibitor SB-3CT is toxic during early hematopoiesis, but ARP-mediated Mmp2 inhibition has no effect on arterial identity or cell death. *Related to Figure 2.*

A) Exposure to 10μM SB-3CT (pan-MMP2/9 inhibitor) during HSPC formation (12-36 hpf) decreased *runx1/cmyb* expression, while 1μM SB-3CT had no effect by WISH analysis.

B) Qualitative phenotypic distribution of embryos scored with high/medium/low *runx1/cmyb* expression in the AGM at 36 hpf (n≥20 embryos/condition).

C) High dose SB-3CT (10μM) treatment (as in S2A) caused major vascular defects and deformities in *Tg(kdrl:gfp)* embryos, suggestive of overall toxicity.

D) Qualitative phenotypic distribution of embryos scored with normal/mild defect/major defect in Flk1:GFP expression (n≥20 embryos/condition).

E) Exposure to high dose SB-3CT (10μM) at a later time point (38-60 hpf), post-HSPC specification and EHT onset, diminished *cmyb* expression in the CHT and caused sustained appearance in the AGM, while low dose (1μM) had less prominent impact by WISH analysis.

F) Qualitative phenotypic distribution of embryos scored with high/medium/low *cmyb* expression in the CHT at 60 hpf (n-value as in 2B).

G) Delayed onset of treatment with SB-3CT (as in S2E) led to minor vascular defects (abnormal vascular branching) in *Tg(kdrl:gfp)* embryos, suggesting embryos better tolerate exposure at later time points.

H) Qualitative phenotypic distribution of embryos scored with normal/mild defect/major defect in Flk1:GFP expression (n-value as in 2D).

I) Exposure to Prinomastat (20μM), ARP-101 (ARP, 10μM), or MMP9-I (5μM) during HSPC formation (12-36 hpf) had no effect on *ephrinB2* expression in the AGM at 36 hpf by WISH analysis (n≥10/condition).

J) Exposure to ARP does not alter the appearance of Acridine Orange (AO) positive (apoptotic) cells in the AGM at 36 hpf compared to controls.

K) Quantification of the number of AO^+ cells in the AGM region in control and ARP treated embryos (DMSO: 3.64 ±2.90; ARP: 3.25 ±2.59; p=0.61, 2-tailed t-test; n≥20 embryos/condition).

Scale bars: 100μm.

Figure S3. Validation of the *Tg(runx1+23$^{(144-378)}$:egfp)* HSPC reporter transgenic zebrafish line and characterization of the effect of Mmp2 inhibition on cell proliferation. *Related to Figure 3.*

A) Genomic DNA sequence corresponding to the murine +23 Runx1 enhancer (black) and the internal 144-378 base pair fragment (Runx1+23$^{(144-378)}$, red).

B) Schematic representation of the Runx1+144:GFP DNA construct used to create the *Tg(runx1+23$^{(144-378)}$:eGFP)* line; a *Tg(runx1+23:egfp)* transgenic reporter genetically similar to the recently published *Tg(runx:egfp)* line (Tamplin et al., 2015) was also created using the full murine enhancer sequence.

C) Representative fluorescence pattern Cd41:GFP^{+}, Runx1+23:GFP^{+} and Runx1+144:GFP^{+} cells in the AGM of transgenic embryos at 36 hpf after treatment with dmPGE2 (10μM; 12-36 hpf) compared to DMSO controls, measured with the same length of exposure time.

D) Representative images of Runx1+144:GFP expression in the CHT (*top*) and thymus (*bottom*) at 84 hpf.

E) Exposure to ARP-101 (ARP, 10μM) from 12-24 hpf does not impact the appearance of proliferating cells in the AGM of *Tg(EF1:mAG-zGEM(1/100); kdrl:dsred)* embryos compared to controls at 24 hpf.

F) Quantification of the number of mAG-zGEM (G2/M)$^{+}$ cells in the AGM of embryos from S3E (DMSO: 34.0 ±18.6; MMP9-I: 32.8 ±9.64, p=0.865, 2-tailed t-test, n≥7 embryos/condition). Error bars: mean ± SD.

Scale bars: 100μm.

Figure S4. Mmp2 inhibition causes an accumulation of fibronectin in the AGM. *Related to Figure 4.*

A) Exposure to SB-3CT (10μM, 32-48 hpf) increased fibronectin staining in the AGM compared to controls at 48 hpf (n≥10 embryos/condition).

B) Vibratome cross-sections show increased fibronectin staining in the posterior cardinal vein (PCV) and ventral wall of the dorsal aorta (DA) with SB-3CT treatment (32-54 hpf) compared to controls; inset

magnifications of boxed regions (from *left panels*) show gray-scale fluorescence of fibronectin (*right*; n≥7 embryos/condition).

Scale bars: 30 (A) and 15μm (B).

Figure S5. Mmp2 inhibition delays HSPC migration to the CHT without impacting circulation. *Related to Figure 5.*

A) *mmp2* mutants display inappropriate *cmyb* expression in the AGM at 72 hpf, phenocopying the effect of ARP- and MO-mediated Mmp2 inhibition.

B) Qualitative phenotypic distribution of total embryos from S5A (*mmp2*$^{+/-}$ incross) scored with normal versus abnormal *cmyb* expression in the AGM at 72 hpf (n≥20 embryos/condition).

C) Embryos exposed to ARP (10μM, 12-48 hpf) showed reduced *cmyb* expression in the CHT, concurrent with enhanced expression in the AGM at 48 hpf, suggesting HSPCs are restrained in colonization of secondary hematopoietic sites with loss of Mmp2 function.

D) Qualitative phenotypic distribution of embryos from S5C scored with normal versus abnormal *cmyb* expression at 48 hpf (n≥20 embryos/condition).

E) *In vivo* imaging of *Tg(kdrl:gfp/gata1a:dsred)* embryos after exposure (12-72 hpf) to ARP, MMP9-I or Prinomastat showed no differences in Gata1^{+} erythrocyte circulation through the Flk1^{+} CHT vasculature compared to controls at 72 hpf (n≥10 embryos/condition).

Scale bars: 100μm.

Figure S6. Mmp9 inhibition impacts HSPC localization and number in the CHT, independent of alterations in cell proliferation. *Related to Figure 6.*

A) *In vivo* imaging of *Tg(-6.0itga2b:egfp)* embryos showed MMP9-I treatment (5μM,12-72 hpf) increased the appearance of Cd41^{+} HSPCs in the CHT region, including preferential accumulation in the anterior (*blue bar*) versus posterior (*orange bar*) half of the hematopoietic niche.

B) Quantification of the phenotype shown in S6A via manual counts of the number of Cd41:GFP^{+} cells per entire CHT region (DMSO: 43.5 ±1.73; MMP9-I: 64.75 ±7.93, *p<0.05, 2-tailed t-test, n≥4 embryos/condition). Error bars: mean ± SD.

C) FACS for Cd41:GFP^{+},Gata1:dsRed^{-} cells (with negative thrombocyte selection) showed no difference in whole embryo HSPC numbers at 72 hpf with MMP9-I exposure (12-72 hpf) compared to control (DMSO: 0.83 ±0.077; MMP9-I: 0.781 ±0.028, p=0.328, 2-tailed t-test, n≥5 embryos/sample, >3 replicates/condition). Error bars: mean ± SD.

D) Quantification of the localization phenotype observed in S6A via manual count Cd41:GFP^{+} HSPCs in each half of the CHT at 72 hpf revealed an increase in the anterior: posterior cell number ratio with Mmp9 (12-72 hpf) inhibition (DMSO: 0.62 ±0.132; MMP9-I: 1.16 ±0.317, *p<0.05, 2-tailed t-test, n-value as in S6B). Error bars: mean ± SD.

E) EdU labeling in *Tg(runx1+23$^{(144-235)}$:egfp)* embryos showed no change in the level of double positive EdU/Runx1+144 staining in the CHT after MMP9-I treatment (24-72 hpf).

F) Qualitative phenotypic distribution of total embryos from S6E scored with high, medium, or low EdU staining level at 72 hpf (n≥20 embryos/condition).

G) pH3 staining in *Tg(runx1+23$^{(144-235)}$:egfp)* embryos showed no alteration in the number of double positive pH3/Runx1+144 cells in the CHT after MMP9-I treatment (24-72 hpf).

H) Quantification of the phenotype in S6G via manual counts of the number of pH3^{+}/Runx1+144:GFP^{+} HSPCs per CHT in control and MMP9-I treated embryos (DMSO: 2.58 ±1.42; MMP9-I: 1.91 ±1.56; p=0.13, 2-tailed t-test; n≥20 embryos/condition). Error bars: mean ± SD.

Scale bars: 100μm.

Figure S7. Mmp9 inhibition does not impact HSPC localization in *cxcl12a* heterozygous mutants.

Related to Figure 7.

A) Exposure of wild-type (WT) sibling controls to MMP9-I (5μM, 12-72 hpf) increased *cmyb* expression in the CHT at 72 hpf; in contrast, while heterozygous loss of *cxcl12a* in *cxcl12a$^{t30516/t30516}$* (*cxcl12a$^{+/-}$*)

embryos had no impact on *cmyb* expression alone, it antagonized the effect of Mmp9 inhibition (n≥20/condition).

B) Qualitative phenotypic distribution of control and MMP9-I treated WT and *cxcl12a*$^{+/-}$ siblings from S7A scored with high/medium/low *cmyb* expression at 72 hpf (n≥20/condition).

Scale bars: 100μm.

Supplemental Figure 1

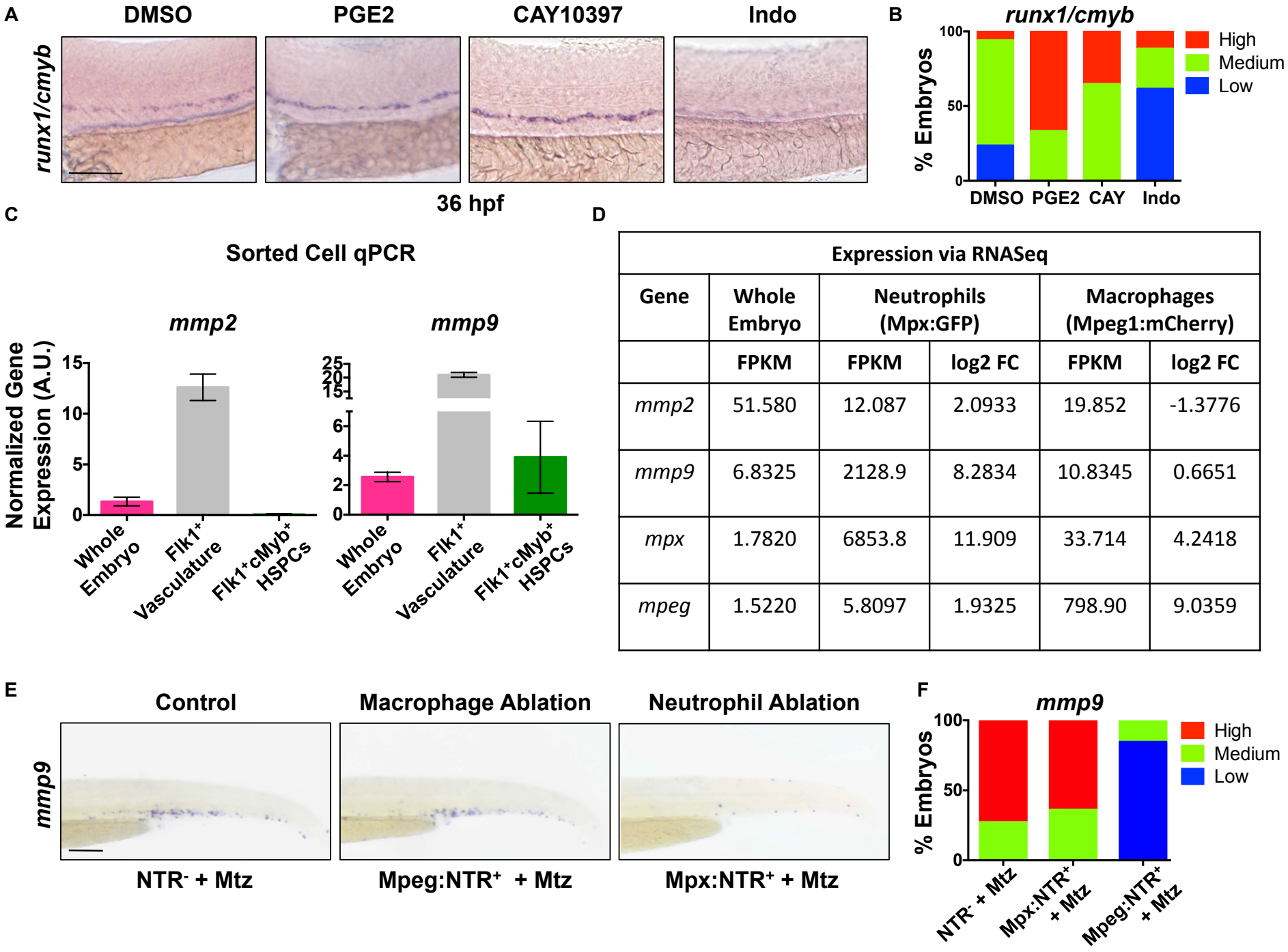

Expression via RNASeq					
Gene	Whole Embryo	Neutrophils (Mpx:GFP)		Macrophages (Mpeg1:mCherry)	
	FPKM	FPKM	log2 FC	FPKM	log2 FC
mmp2	51.580	12.087	2.0933	19.852	-1.3776
mmp9	6.8325	2128.9	8.2834	10.8345	0.6651
mpx	1.7820	6853.8	11.909	33.714	4.2418
mpeg	1.5220	5.8097	1.9325	798.90	9.0359

Supplemental Figure 2

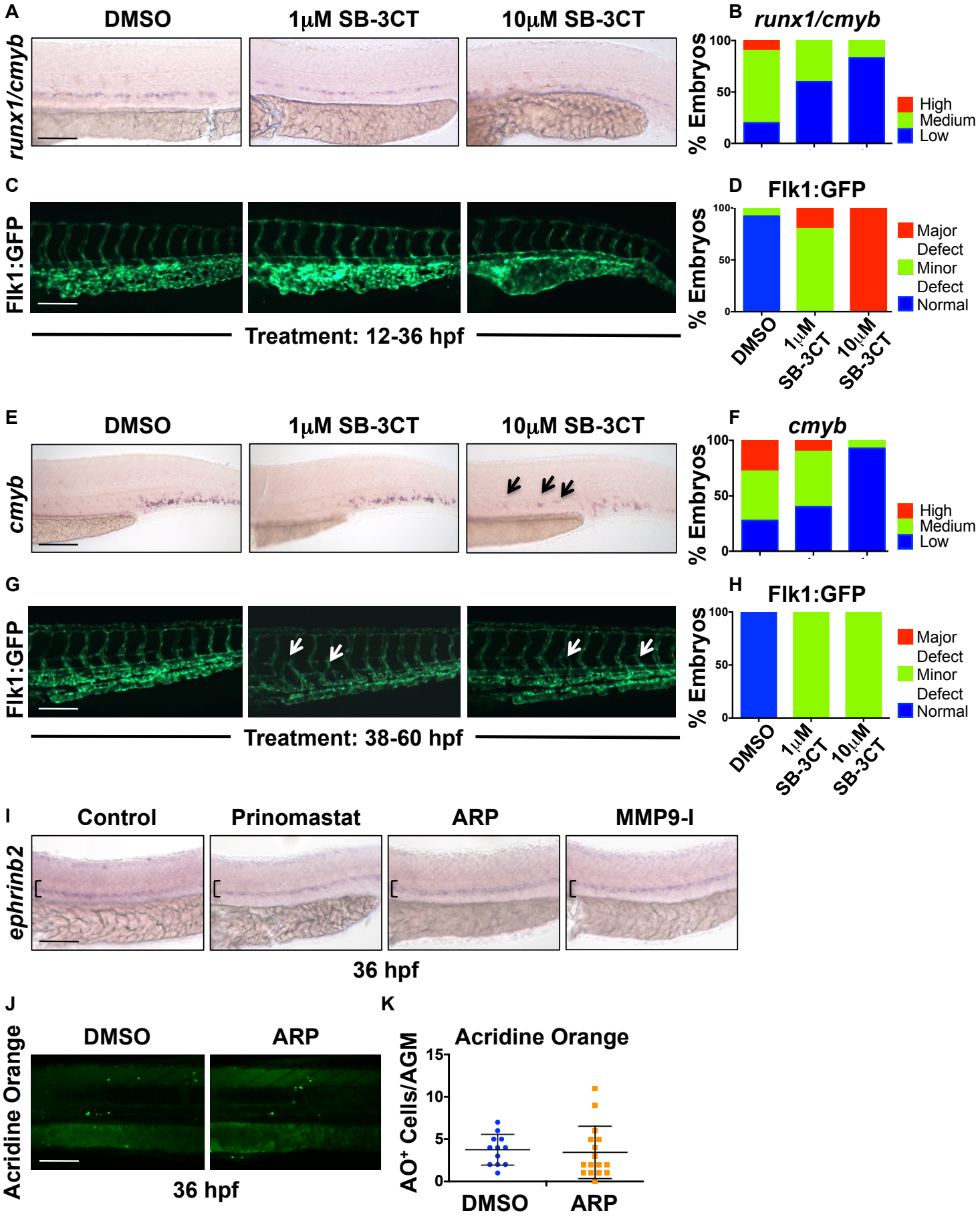

Supplemental Figure 3

A

tgggggtgggaggtgtaagttccacccccaccttcctgacacgctcctg
aaccctggccactgcacctgctaggttctcacttctctgggaagcatcta
gaaacaggacctctcacccacccctcccggctgggctctagggtggggcc
ctcactacctcttttcttctcaaagagcctgggatgctgacagcctcaga
tggaggcatcctgtttgtcgaaaaataaaccggcagttgaagccgggttg
caagagcgagaaaaccgcaggcctgcgcgccactgataacgtgggcagct
tgcttttgcagcagttcctagctgcagcggccctgtgaaggcctgtgtca
ccgcctccctcctgtctcctcctcacaccatccctccatcgctccttgc
tggctctaccagccacttgctggacccttcagccactgggaccattgctt
tccataaaaaactccttagtgcagtgcagagctgatcagagggtagcagg
gaaccctgacgcctgatgggttgctgacacctggg

B

C

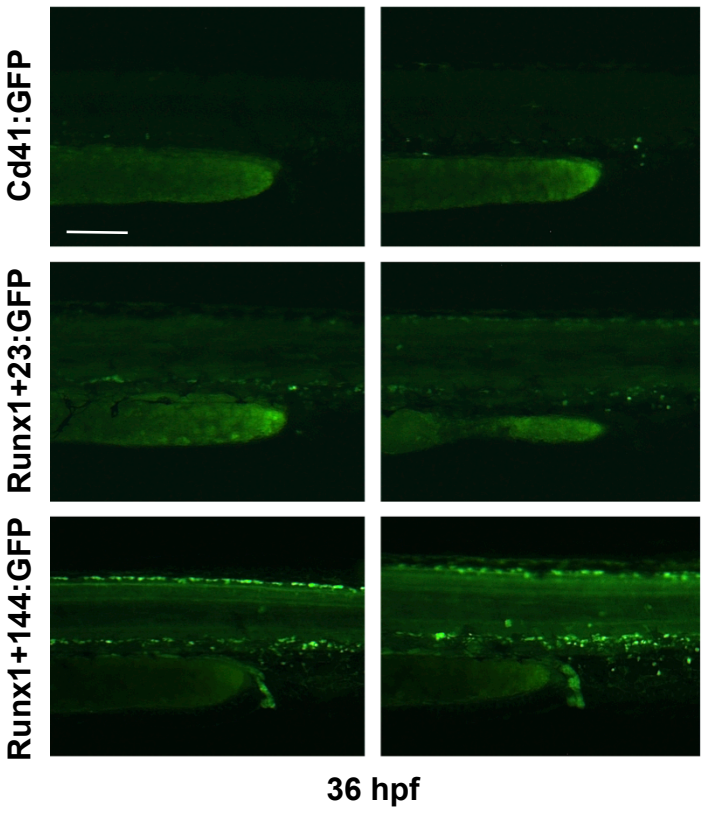

D

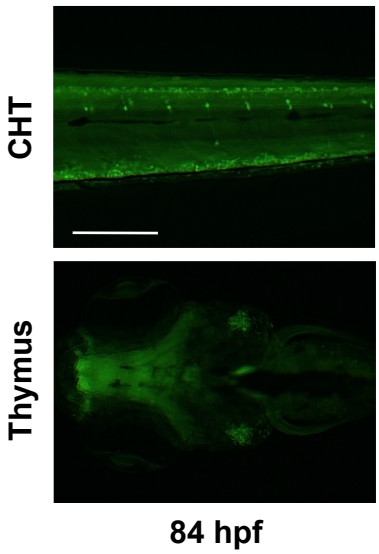

E

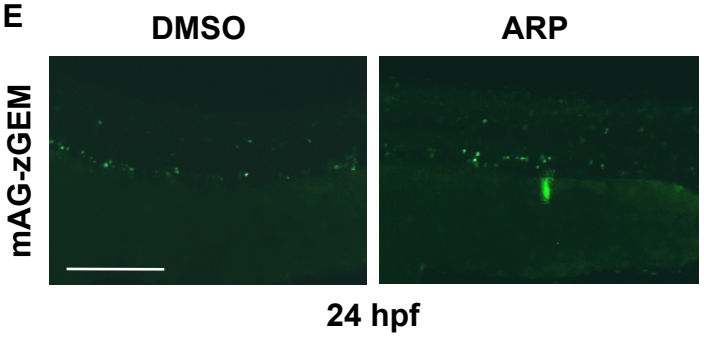

F

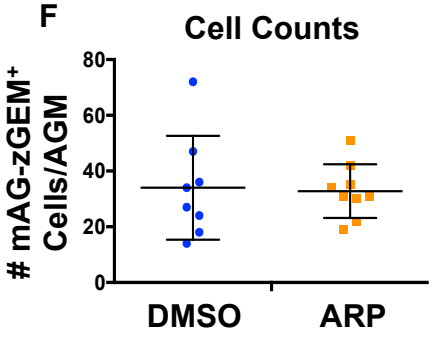

Supplemental Figure 4

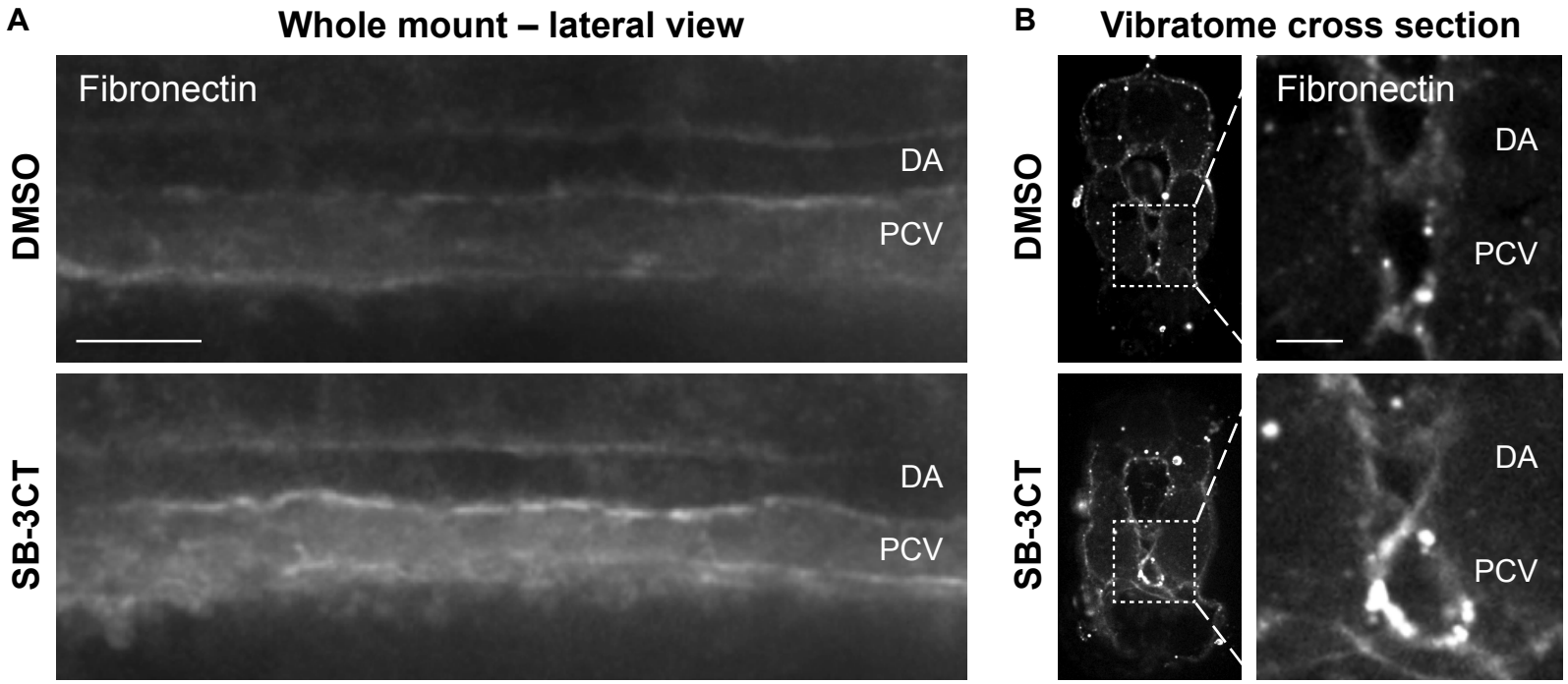

Supplemental Figure 5

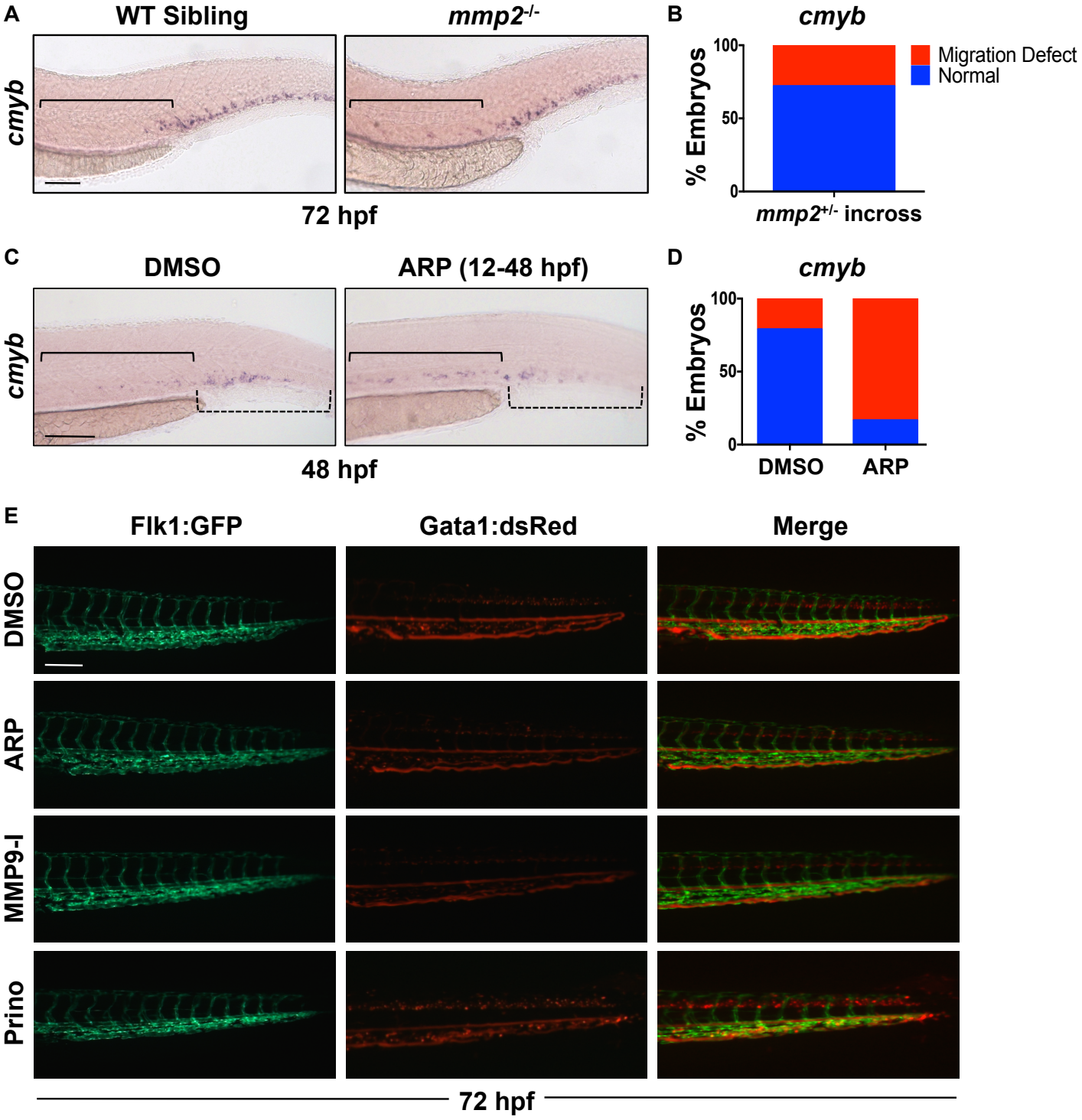

Supplemental Figure 6

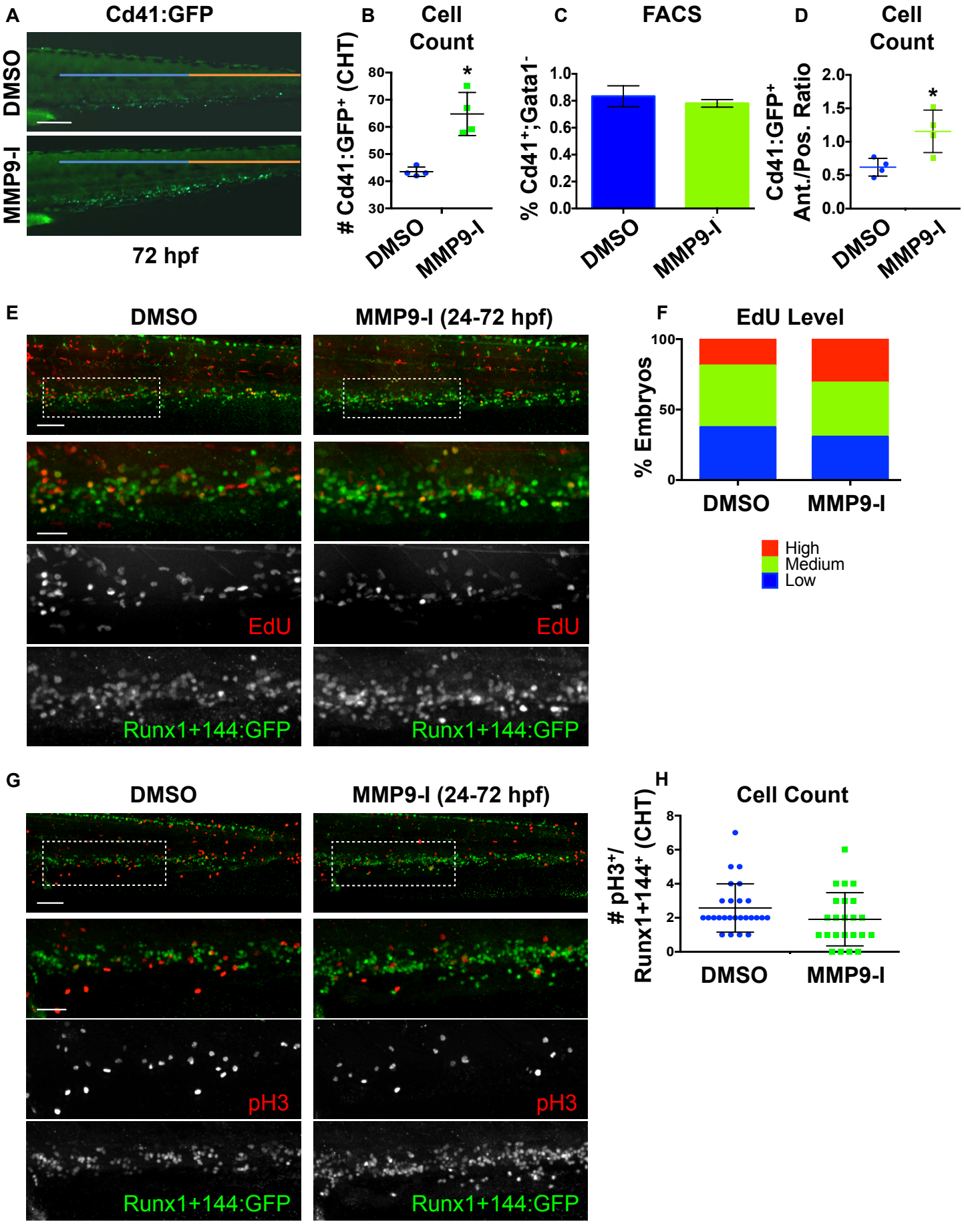

Supplemental Figure 7

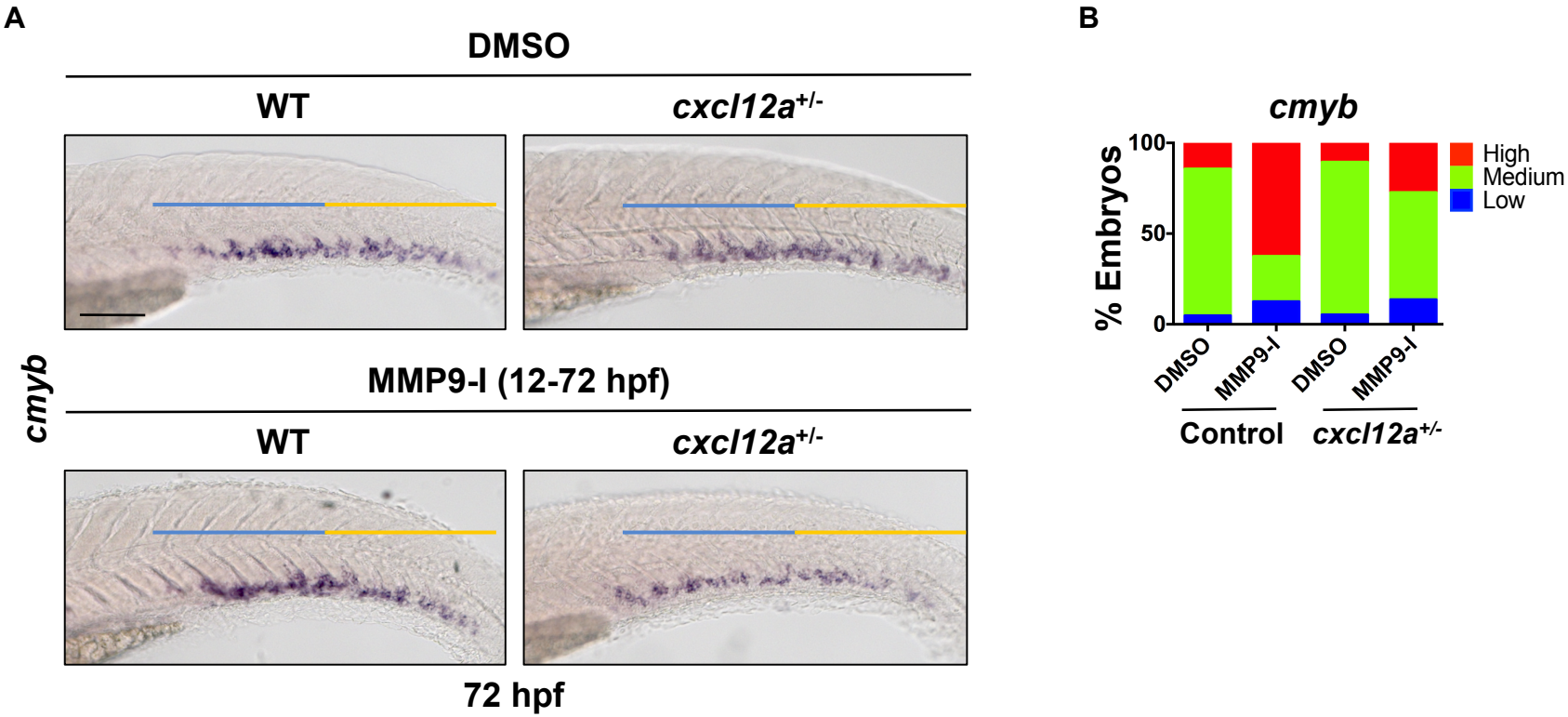

SUPPLEMENTAL EXPERIMENTAL PROCEDURES

Transgenic and Mutant Zebrafish Lines (related to Zebrafish Husbandry)

Official Line Name	**Common Name**	**Reference**
Tg(-6.0itga2b:egfp)	Cd41:GFP	(Bertrand et al., 2008)
Tg(kdrl:gfp)	Flk1:GFP	(Choi et al., 2007)
Tg(kdrl:dsred2)	Flk1:dsRed	(Kikuchi et al., 2011)
Tg(cmyb:egfp)	cMyb:GFP	(North et al., 2007)
Tg(gata1a:dsRed)	Gata1:dsRed	(Traver et al., 2003)
Tg(runx+23$^{(144-378)}$:egfp)	Runx1+144:GFP	*see description below*
Tg(runx1P2:egfp)	Runx1:GFP	(Lam et al., 2010)
fn1a$^{tl43c/tl43c}$	*natter, fibronectin* mutant	(Trinh and Stainier, 2004)
Tg(hsp70l:cxcl12b-egfp)	Hsp70:Cxcl12b	(Li et al., 2005)
cxcl12a$^{t30516/t30516}$	*medusa, cxcl12a* mutant	(Valentin et al., 2007)
mmp2^{hu10535}	*mmp2* mutant	(Kok et al., 2015)
Tg(mpeg1:gal4;uas:nfsb-mcherry)	Mpeg1:NTR	(Davison et al., 2007; Ellett et al., 2011)
Tg(mpx:gal4;uas:nfsb-mcherry)	Mpx:NTR	(Davison et al., 2007; Robertson et al., 2014)
Tg(EF1:mAG-zGem(1/100))rw0410h)	mAG-zGEM	(Sugiyama et al., 2009)
Tg(runx1+23:egfp)	Runx1+23:GFP	*see description below* [*similar to* (Tamplin et al., 2015)]
Tg(mpeg1:mcherry)	Mpeg1:mCherry	(Ellett et al., 2011)
Tg(mpx:egfp)	Mpx:GFP	(Renshaw et al., 2006)
Tg(rag2:dsred)zf411	Rag2:dsRed	(Ma et al., 2012)

Morpholino Sequences (related to Morpholino Injections)

Gene	Morpholino	Reference
mmp2	5' - GTGGCGAACAGCCCTTTCAGACGTG - 3'	(Coyle et al., 2008)
mmp9	5'-CGCCAGGACTCCAAGTCTCATTTTG- 3'	(Volkman et al., 2010)
cxcl12a	5'-CTACTACGATCACTTTGAGATCCAT-3'	(Doitsidou et al., 2002)

qPCR Primers (related to RNA Extraction and qRT-PCR)

Gene	Forward	Reverse	Reference
mmp2	GCTGTTCCCGATGACCTAGA	GCTGTCATTTCTGGCCATTT	
mmp9	TTGCCTTTTCCTCTCTGCAT	TCATGATCTCTGCGAAGTGG	(Esain et al., 2015)
18s	TCGCTAGTTGGCATCGTTTAT	CGGAGGTTCGAAGACGATCA	(Esain et al., 2015)

Small Molecules

Drug	Target	Dose	Supplier	Reference
ARP-101	MMP2	10μM	Tocris	
MMP9-I	MMP9	5μM	Merck Millipore	
Prinomastat	MMP2/MMP9	20μM	Sigma-Aldrich	
SB-3CT	MMP2/MMP9	1, 10μM	Sigma-Aldrich	(Travnickova et al., 2015)
dmPGE2		10μM	Cayman Chemical	(North et al., 2007)
Indomethacin	Cyclooxygenase 1/2	10μM	Sigma-Aldrich	(North et al., 2007)
CAY10397	PGDH	10μM	Cayman Chemical	(Nissim et al., 2014)

Antibodies

Antibody	Species	Source	Catalog Number
Fibronectin	Rabbit	Sigma-Aldrich	F3648
Anti-phospho-Histone H3 ($pSer^{10}$)	Rabbit	EMD Millipore	06-570
GFP	Rabbit	Millipore (Sigma-Aldrich)	AB3080
GFP	Chicken	GeneTex	GTX13970
Anti-rabbit IgG, Alexa Fluor 488	Goat	Molecular Probes (Thermo Fisher)	A-11034

Anti-rabbit IgG, Alexa Fluor 568	Goat	Molecular Probes (Thermo Fisher)	A-11011
Anti-chicken IgG, Alexa Fluor 488	Goat	Molecular Probes (Thermo Fisher)	A-11039

Generation of the Tg(runx1+23*(144-378)*:egfp) HSPC reporter transgenic zebrafish line

A 235 base pair fragment corresponding to region 144-378 of +23 Runx1 murine enhancer (Nottingham, et al. 2007), as well as the full enhancer region, were amplified from mouse genomic DNA with the following primers: Runx1+144Fwd-5'-GGGGCCCTCACTACCTCTTTTCTTCTC-3' and Runx1+144Rev-5'-GTGTGAGGAGGAGACAGGAAGAAGGGAGGC-3' or Runx1+23Fwd-5' -GGGGGTGGGAGGTGTAAGTTC-3' and Runx1+23Rev-5' –CCAGGTGTCAGCAACCCATC-3', and cloned into pT2-cfos-EGFP (Fisher et al., 2006). *Tg(runx1+23:egfp)* and *Tg(runx1+23$^{(144-378)}$:egfp)* transgenic fish were generated by co-injection of the Tol2-transposase mRNA (Kwan et al., 2007) into 1-cell stage embryos and transgenic F_0 founders were identified by eGFP expression in the AGM.

SUPPLEMENTAL REFERENCES

Bertrand, J.Y., Kim, A.D., Teng, S., and Traver, D. (2008). CD41+ cmyb+ precursors colonize the zebrafish pronephros by a novel migration route to initiate adult hematopoiesis. Development *135*, 1853–1862.

Choi, J., Dong, L., Ahn, J., Dao, D., Hammerschmidt, M., and Chen, J.-N. (2007). FoxH1 negatively modulates flk1 gene expression and vascular formation in zebrafish. Developmental Biology *304*, 735–744.

Coyle, R.C., Latimer, A., and Jessen, J.R. (2008). Membrane-type 1 matrix metalloproteinase regulates cell migration during zebrafish gastrulation: Evidence for an interaction with non-canonical Wnt signaling. Experimental Cell Research *314*, 2150–2162.

Davison, J.M., Akitake, C.M., Goll, M.G., Rhee, J.M., Gosse, N., Baier, H., Halpern, M.E., Leach, S.D.,

and Parsons, M.J. (2007). Transactivation from Gal4-VP16 transgenic insertions for tissue-specific cell labeling and ablation in zebrafish. Developmental Biology *304*, 811–824.

Doitsidou, M., Reichman-Fried, M., Stebler, J., Köprunner, M., Dörries, J., Meyer, D., Esguerra, C.V., Leung, T., and Raz, E. (2002). Guidance of primordial germ cell migration by the chemokine SDF-1. Cell *111*, 647–659.

Ellett, F., Pase, L., Hayman, J.W., Andrianopoulos, A., and Lieschke, G.J. (2011). mpeg1 promoter transgenes direct macrophage-lineage expression in zebrafish. Blood *117*, e49–e56.

Esain, V., Kwan, W., Carroll, K.J., Cortes, M., Liu, S.Y., Frechette, G.M., Sheward, L.M.V., Nissim, S., Goessling, W., and North, T.E. (2015). Cannabinoid Receptor-2 Regulates Embryonic Hematopoietic Stem Cell Development via Prostaglandin E2 and P-Selectin Activity. Stem Cells *33*, 2596–2612.

Fisher, S., Grice, E.A., Vinton, R.M., Bessling, S.L., Urasaki, A., Kawakami, K., and McCallion, A.S. (2006). Evaluating the biological relevance of putative enhancers using Tol2 transposon-mediated transgenesis in zebrafish. Nat Protoc *1*, 1297–1305.

Goessling, W., North, T.E., Loewer, S., Lord, A.M., Lee, S., Stoick-Cooper, C.L., Weidinger, G., Puder, M., Daley, G.Q., Moon, R.T., et al. (2009). Genetic Interaction of PGE2 and Wnt Signaling Regulates Developmental Specification of Stem Cells and Regeneration. Cell *136*, 1136–1147.

Kikuchi, K., Holdway, J.E., Major, R.J., Blum, N., Dahn, R.D., Begemann, G., and Poss, K.D. (2011). Retinoic Acid Production by Endocardium and Epicardium Is an Injury Response Essential for Zebrafish Heart Regeneration. Developmental Cell *20*, 397–404.

Kok, F.O., Shin, M., Ni, C.-W., Gupta, A., Grosse, A.S., van Impel, A., Kirchmaier, B.C., Peterson-Maduro, J., Kourkoulis, G., Male, I., et al. (2015). Reverse Genetic Screening Reveals Poor Correlation between Morpholino-Induced and Mutant Phenotypes in Zebrafish. Developmental Cell *32*, 97–108.

Kwan, K.M., Fujimoto, E., Grabher, C., Mangum, B.D., Hardy, M.E., Campbell, D.S., Parant, J.M., Yost, H.J., Kanki, J.P., and Chien, C.-B. (2007). The Tol2kit: A multisite gateway-based construction kit forTol2 transposon transgenesis constructs. Developmental Dynamics *236*, 3088–3099.

Lam, E.Y.N., Hall, C.J., Crosier, P.S., Crosier, K.E., and Flores, M.V. (2010). Live imaging of Runx1 expression in the dorsal aorta tracks the emergence of blood progenitors from endothelial cells. Blood *116*, 909–914.

Li, Q., Shirabe, K., Thisse, C., Thisse, B., Okamoto, H., Masai, I., and Kuwada, J.Y. (2005). Chemokine signaling guides axons within the retina in zebrafish. J. Neurosci. *25*, 1711–1717.

Ma, D., Wang, L., Wang, S., Gao, Y., Wei, Y., and Liu, F. (2012). Foxn1 maintains thymic epithelial cells to support T-cell development via mcm2 in zebrafish. Proc. Natl. Acad. Sci. U.S.a. *109*, 21040–21045.

Nissim, S., Sherwood, R.I., Wucherpfennig, J., Saunders, D., Harris, J.M., Esain, V., Carroll, K.J., Frechette, G.M., Kim, A.J., Hwang, K.L., et al. (2014). Prostaglandin E2 Regulates Liver versus Pancreas Cell-Fate Decisions and Endodermal Outgrowth. Developmental Cell *28*, 423–437.

North, T.E., Goessling, W., Walkley, C.R., Lengerke, C., Kopani, K.R., Lord, A.M., Weber, G.J., Bowman, T.V., Jang, I.-H., Grosser, T., et al. (2007). Prostaglandin E2 regulates vertebrate haematopoietic stem cell homeostasis. Nature *447*, 1007–1011.

Nottingham, W.T., Jarratt, A., Burgess, M., Speck, C.L., Cheng, J.-F., Prabhakar, S., Rubin, E.M., Li, P.-S., Sloane-Stanley, J., Kong-A-San, J., et al. (2007). Runx1-mediated hematopoietic stem-cell emergence is controlled by a Gata/Ets/SCL-regulated enhancer. Blood *110*, 4188–4197.

Renshaw, S.A., Loynes, C.A., Trushell, D.M.I., Elworthy, S., Ingham, P.W., and Whyte, M.K.B. (2006). A transgenic zebrafish model of neutrophilic inflammation. Blood *108*, 3976–3978.

Robertson, A.L., Holmes, G.R., Bojarczuk, A.N., Burgon, J., Loynes, C.A., Chimen, M., Sawtell, A.K., Hamza, B., Willson, J., Walmsley, S.R., et al. (2014). A zebrafish compound screen reveals modulation of neutrophil reverse migration as an anti-inflammatory mechanism. Sci Transl Med *6*, 225ra29–225ra29.

Sugiyama, M., Sakaue-Sawano, A., Iimura, T., Fukami, K., Kitaguchi, T., Kawakami, K., Okamoto, H., Higashijima, S.-I., and Miyawaki, A. (2009). Illuminating cell-cycle progression in the developing zebrafish embryo. Proc. Natl. Acad. Sci. U.S.a. *106*, 20812–20817.

Tamplin, O.J., Durand, E.M., Carr, L.A., Childs, S.J., Hagedorn, E.J., Li, P., Yzaguirre, A.D., Speck, N.A., and Zon, L.I. (2015). Hematopoietic Stem Cell Arrival Triggers Dynamic Remodeling of the Perivascular Niche. Cell *160*, 241–252.

Traver, D., Paw, B.H., Poss, K.D., Penberthy, W.T., Lin, S., and Zon, L.I. (2003). Transplantation and in vivo imaging of multilineage engraftment in zebrafish bloodless mutants. Nat Immunol *4*, 1238–1246.

Travnickova, J., Tran Chau, V., Julien, E., Mateos-Langerak, J., Gonzalez, C., Lelièvre, E., Lutfalla, G., Tavian, M., and Kissa, K. (2015). Primitive macrophages control HSPC mobilization and definitive haematopoiesis. Nat Commun *6*, 6227.

Trinh, L.A., and Stainier, D.Y.R. (2004). Fibronectin Regulates Epithelial Organization during Myocardial Migration in Zebrafish. Developmental Cell *6*, 371–382.

Valentin, G., Haas, P., and Gilmour, D. (2007). The Chemokine SDF1a Coordinates Tissue Migration through the Spatially Restricted Activation of Cxcr7 and Cxcr4b. Current Biology *17*, 1026–1031.

Volkman, H.E., Pozos, T.C., Zheng, J., Davis, J.M., Rawls, J.F., and Ramakrishnan, L. (2010). Tuberculous Granuloma Induction via Interaction of a Bacterial Secreted Protein with Host Epithelium. Science *327*, 466–469.